Eur. J. Mineral.
2014, **26**, 427–437

Mapiquiroite, $(Sr,Pb)(U,Y)Fe_2(Ti,Fe^{3+})_{18}O_{38}$, a new member of the crichtonite group from the Apuan Alps, Tuscany, Italy

Cristian BIAGIONI[1,*], Paolo ORLANDI[1,2], Marco PASERO[1], Fabrizio NESTOLA[3] and Luca BINDI[4]

[1] Dipartimento di Scienze della Terra, Università di Pisa, Via S. Maria 53, 56126 Pisa, Italy
*Corresponding author, e-mail: biagioni@dst.unipi.it
[2] Istituto di Geoscienze e Georisorse, Consiglio Nazionale delle Ricerche, Via Moruzzi 1, 56124 Pisa, Italy
[3] Dipartimento di Geoscienze, Università di Padova, Via Gradenigo 6, 35131 Padova, Italy
[4] Dipartimento di Scienze della Terra, Università di Firenze, Via G. La Pira 4, 50121 Firenze, Italy

Abstract: Mapiquiroite, $(Sr,Pb)(U,Y)Fe_2(Ti,Fe^{3+})_{18}O_{38}$, was identified as a new mineral from the baryte + pyrite + iron oxide ores of Buca della Vena (BdV) and Monte Arsiccio (MA) mines, Apuan Alps, Tuscany, Italy. At BdV, mapiquiroite occurs as complex rhombohedral or tabular pseudo-hexagonal crystals, up to 1 mm in size, black in colour, with a sub-metallic lustre, in quartz + 'adularia' + baryte veins embedded in schists, in association with allanite-(Ce), anatase, destinezite, gypsum, monazite-(Ce), pyrite, rutile, and 'tourmaline'; at MA, mapiquiroite forms tabular pseudo-hexagonal crystals, up to 5 mm in size, in quartz + carbonate veins embedded in magnetite-rich dolostones, in association with baryte, boulangerite, derbylite, siderite, and sphalerite. Under the microscope, mapiquiroite is blackish in colour, weakly bireflectant, and non-pleochroic. Internal reflections are absent. Anisotropism is distinct, without characteristic rotation tints. Minimum and maximum reflectance data for COM wavelengths [λ (nm), R_{air} (%); data for the specimens from BdV and MA, respectively] are: 471.1, 17.0/17.2 and 17.7/18.0; 548.3, 16.7/17.0 and 17.6/17.8; 586.6, 16.4/16.7 and 17.3/17.7; 652.3, 16.1/16.3 and 17.0/17.3. Vickers hardness is 750 $kg \cdot mm^{-2}$ and 782 $kg \cdot mm^{-2}$ for specimens from BdV and MA, respectively, corresponding to a Mohs' hardness ~ 6. The chemical data point to the formulae $(Sr_{0.533}La_{0.176}Pb_{0.105}Na_{0.030}Ca_{0.026})_{\Sigma=0.870}(U_{0.407}Ce_{0.101}Y_{0.205}Mn_{0.072})_{\Sigma=0.785}Fe^{3+}_{2.000}(Ti_{12.423}Fe^{3+}_{3.345}Cr_{1.624}V^{5+}_{0.129}Al_{0.032}Sn_{0.013}Nb_{0.007})_{\Sigma=17.573}O_{38}$ (BdV) and $(Sr_{0.312}Pb_{0.248}Na_{0.019}Ca_{0.014}La_{0.009})_{\Sigma=0.602}(U_{0.858}Y_{0.070}Ce_{0.021}Mn_{0.005})_{\Sigma=0.954}(Fe^{3+}_{1.695}Zn_{0.305})_{\Sigma=2.000}(Ti_{12.070}Fe^{3+}_{4.987}V^{5+}_{0.372}Al_{0.030}Nb_{0.030}Cr_{0.015}Sn_{0.001})_{\Sigma=17.505}O_{38}$ (MA). Mapiquiroite is trigonal, $R\bar{3}$, with *a* 10.3719(7), *c* 20.875(1) Å, *V* 1944.8(2) Å^3 and *a* 10.3854(3), *c* 20.8942(6) Å, *V* 1951.7(1) Å^3 for the specimens from BdV and MA, respectively. The crystal structures of mapiquiroite from these two occurrences were refined to $R_1 = 0.028$ and 0.032, respectively. Mapiquiroite is isostructural with other members of the crichtonite group. The name *mapiquiroite* honours four Italian mineral collectors, Riccardo Mazzanti, Luigi Pierotti, Ugo Quilici, and Moreno Romani for their contribution to the study of the mineralogy of baryte + pyrite + iron oxide deposits from the Apuan Alps.

Key-words: mapiquiroite, crichtonite group, new mineral, strontium uranium iron titanate, crystal structure, Buca della Vena, Monte Arsiccio, Apuan Alps, Tuscany, Italy.

1. Introduction

Since the mid 1990s, baryte + pyrite + iron oxide ore deposits from the Apuan Alps have provided the systematic mineralogy with an exceptional series of rare or new minerals. Buca della Vena, Fornovolasco, Monte Arsiccio and Pollone mines are indeed the type localities for sixteen mineral species, thus testifying to the huge scientific importance of this kind of ore deposits, whose mineralogy is still far from being fully described.

Nowadays, the most interesting locality is represented by the Monte Arsiccio mine; its mineralogy is currently under study and a number of rare phases have been identified: mannardite (Biagioni *et al*., 2009), cymrite and benstonite (Biagioni & Orlandi, 2010), two new Tl-Pb sulphosalts [boscardinite and protochabournéite (Orlandi *et al*., 2012, 2013)], together with a series of very rare Tl-Hg-As sulphosalts (Biagioni *et al*., 2013a, b, 2014). During the study of samples from Monte Arsiccio, a new member of the crichtonite group was found, characterized by a high U content.

The identification of a crichtonite-group mineral at Monte Arsiccio (hereafter MA) led us to reinvestigate another phase of the crichtonite group found in quartz + 'adularia' + baryte veins embedded in the tourmaline- and pyrite-rich schists of the southern part of the Buca della Vena mine (hereafter BdV) and provisionally identified as 'dessauite'. Actually, dessauite-(Y) was found at BdV but in a different kind of occurrence, that is in carbonate veins embedded in the dolostone. Chemical analyses clearly indicated that the

0935-1221/14/0026-2382 $ 4.95
DOI: 10.1127/0935-1221/2014/0026-2382

specimens from the two localities are the same mineral phase, which can be considered either as the U-analogue of dessauite-(Y) or the Sr-analogue of cleusonite.

The new mineral species and its name were approved by the IMA-CNMNC (No. 2013–010). The holotype specimens of mapiquiroite are deposited in the mineralogical collection of the Museo di Storia Naturale, Università di Pisa, Via Roma 79, Calci, Pisa, Italy, under catalogue number 18837 (specimen from BdV) and 19650 (specimen from MA). The name honours four Italian mineral collectors for their contribution to the knowledge of the mineralogy of the hydrothermal deposits from Apuan Alps and in particular of the baryte + pyrite + iron oxide ores: Riccardo Mazzanti (b. 1953), Luigi Pierotti (b. 1953), Ugo Quilici (b. 1946), and Moreno Romani (b. 1949). Mapiquiroite is the acronym from their surnames: MAzzanti, PIerotti, QUIlici, and ROmani. Luigi Pierotti, Ugo Quilici, and Moreno Romani provided us with the first specimens of grumiplucite (Orlandi *et al.*, 1998), pellouxite (Orlandi *et al.*, 2004a), rouxelite (Orlandi *et al.*, 2005), oxycalcioroméite (Biagioni *et al.*, 2013c), and mapiquiroite (this work). Riccardo Mazzanti gave us the first specimens of boscardinite (Orlandi *et al.*, 2012) and protochabournéite (Orlandi *et al.*, 2013).

2. Occurrence and mineral description

The geological settings of the BdV and MA mines have been already described (*e.g.*, Benvenuti *et al.*, 1986; Costagliola *et al.*, 1990). Both deposits are formed by conformable ore bodies hosted at the contact between a metasiliclastic-metavolcanic sequence, known as Scisti di Fornovolasco Formation (Pandeli *et al.*, 2004), and Triassic dolostones (Grezzoni Formation).

At Buca della Vena, mapiquiroite was found in vugs of quartz + ‘adularia’ + baryte veins embedded in tourmaline- and pyrite-rich schists, in the southern part of the mine (Fig. 1a). Mapiquiroite is very rare and occurs as rhombohedral or tabular pseudohexagonal crystals, black in colour, with a sub-metallic lustre, up to 1 mm in size (Fig. 2a). In the same veins, allanite-(Ce), anatase, destinezite, gypsum, monazite-(Ce), pyrite, rutile and ‘tourmaline’ occur.

At Monte Arsiccio, mapiquiroite was discovered along an inclined shaft connecting the Sant’Olga tunnel to the completely collapsed fifth sub-level of the Sant’Anna tunnel. The magnetite-rich dolostone is cut by quartz + carbonate veins and by a system of sub-horizontal fractures hosting good specimens of derbylite and stibivanite (Fig. 1b). During the sampling of this occurrence, tabular pseudohexagonal pitch black sub-metallic crystals, up to 5 mm in size, strictly associated with derbylite and sphalerite, embedded in quartz, were observed (Fig. 2b). Only few specimens were collected and only one was made available for the mineralogical characterization. In the same veins, baryte, Ba-rich feldspar (‘hyalophane’), boulangerite, galena, and siderite were identified.

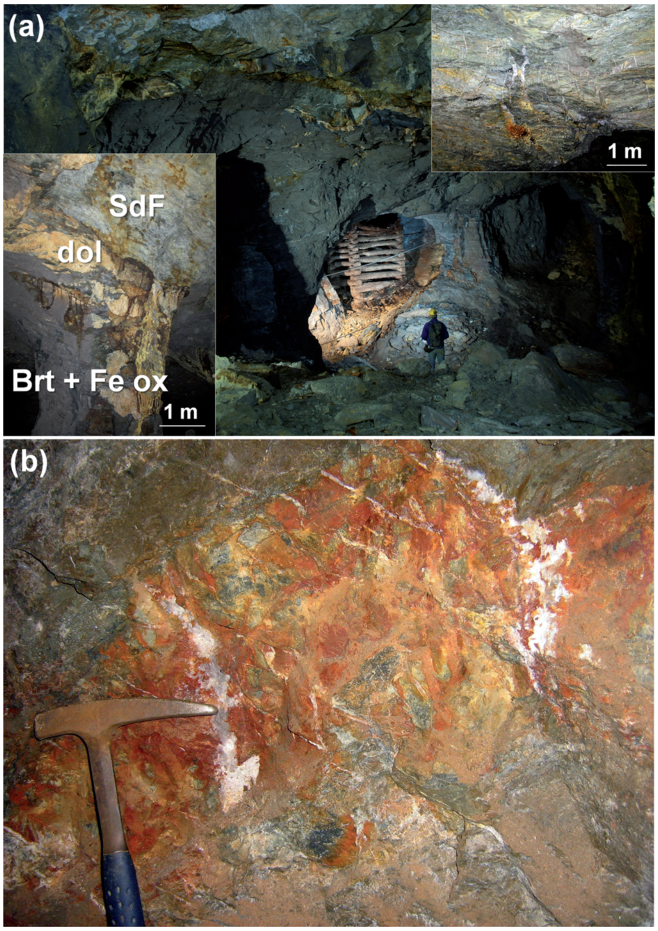

Fig. 1. Occurrence of mapiquiroite at the Buca della Vena mine (BdV) and Monte Arsiccio mine (MA). In (a), the southern part of the BdV mine, with the exploitation voids. Mapiquiroite was found in the collapsed blocks on the floor. Upper right: quartz veins embedded in schists on the roof of the exploitation void. Bottom left: SdF = Scisti di Fornovolasco Formation, dol = dolostone lenses at the contact between the ore body and the schists or within the former, Brt + Fe ox = orebody formed by granoblastic baryte + iron oxides (hematite, magnetite). In (b), the occurrence of mapiquiroite at MA, in quartz veins embedded in iron-rich dolostones. (online version in colour)

2.1. Optical and physical properties

Mapiquiroite is brittle, with an irregular fracture. The streak is black. The Vickers hardness (carried out with a load of 500 g) is 782 kg·mm^{-2} (range 765–797 kg·mm^{-2}, six measurements) and 750 kg·mm^{-2} (range 722–764 kg·mm^{-2}, eight measurements) for samples from MA and BdV, respectively. These data correspond to a Mohs’ hardness of $\sim$ 6. Density was not measured owing to the low amount of available material; calculated densities, based on the empirical formulae and unit-cell parameters from annealed-single-crystal data, are 4.843 g·cm^{-3} (MA) and 4.670 g·cm^{-3} (BdV).

In plane-polarized incident light, mapiquiroite from both occurrences is blackish in colour, weakly bireflectant, and non-pleochroic. Internal reflections were not observed. Between crossed polars, mapiquiroite is anisotropic, without characteristic tints. The reflectance was measured in air

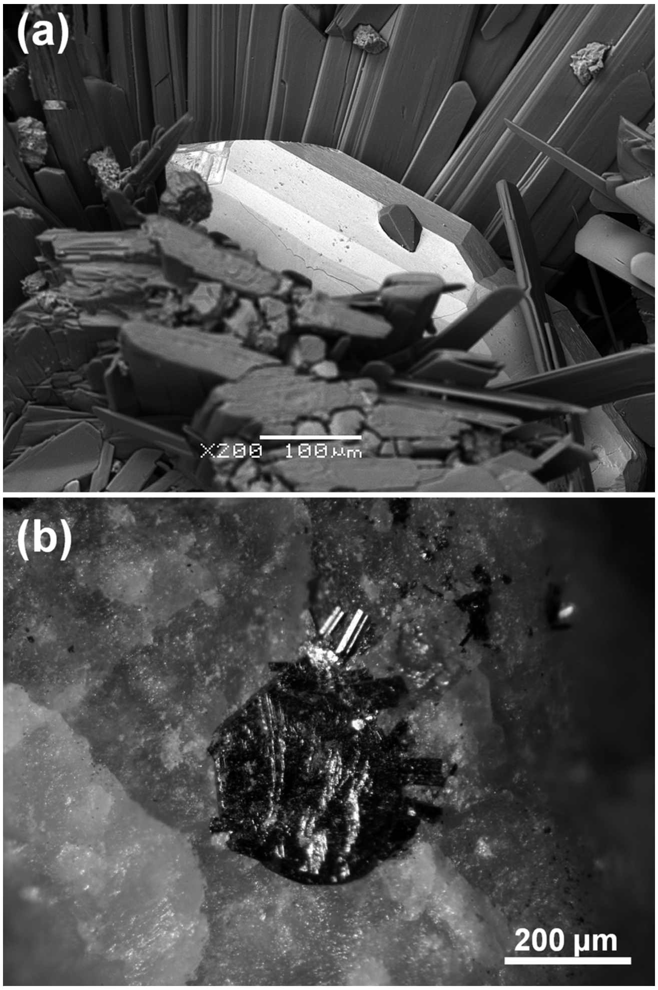

Fig. 2. Specimens of mapiquiroite from BdV (a, scanning electron microscope image) and MA (b, photomicrograph). In (a) mapiquiroite is associated with gypsum. In (b), mapiquiroite forms a tabular pseudo-hexagonal crystal associated with black prismatic crystals of derbylite, in quartz matrix.

using an MPM-200 Zeiss microphotometer equipped with a MSP-20 system processor on a Zeiss Axioplan ore microscope. The filament temperature was approximately 3350 K. Readings were taken for specimens and standard (SiC) maintained under the same focus conditions. The diameter of the circular measuring area was 0.1 mm. Reflectance percentages ($R_{\min}$ and $R_{\max}$) are given in Table 1.

2.2. Chemical data

Preliminary qualitative chemical analyses were performed using a Phillips XL30 scanning electron microscope equipped with an EDAX DX4 system. The only elements with $Z > 9$ detected in mapiquiroite are Sr, Pb, Fe, Ti, and U for the specimen from MA; the same elements plus Cr were detected in the specimen from BdV.

Electron-microprobe analyses were carried on unheated crystals with a Cameca SX50 instrument using the following analytical conditions: accelerating voltage 20 kV, beam current 20 nA, beam size 2 µm. Counting time for one spot analysis was 10 s per peak. Standards (element, emission line) are: albite (Na $K\alpha$); diopside (Ca $K\alpha$); Al_2O_3 (Al $K\alpha$); vanadinite (V $K\alpha$); $MnTiO_3$ (Ti $K\alpha$; Mn $K\alpha$); Cr_2O_3 (Cr $K\alpha$); Fe_2O_3 (Fe $K\alpha$); celestine (Sr $L\alpha$); REE-glass named Ree3–20 (Y $L\alpha$; La $L\alpha$; Ce $L\alpha$); metallic niobium (Nb $L\alpha$); SnO_2 (Sn $L\alpha$); PbS (Pb $M\alpha$); UO_2 (U $M\alpha$). Analytical data are given in Table 2. The empirical formulae, based on 38 oxygen atoms per formula unit (apfu), are $(Sr_{0.533}La_{0.176}Pb_{0.105}Na_{0.030}Ca_{0.026})_{\Sigma=0.870}$ $(U_{0.407}Ce_{0.101}Y_{0.205}Mn_{0.072})_{\Sigma=0.785}$ $Fe^{3+}{}_{2.000}$ $(Ti_{12.423}Fe^{3+}{}_{3.345}Cr_{1.624}V^{5+}{}_{0.129}Al_{0.032}Sn_{0.013}Nb_{0.007})_{\Sigma=17.573}O_{38}$ (BdV) and $(Sr_{0.312}Pb_{0.248}Na_{0.019}Ca_{0.014}La_{0.009})_{\Sigma=0.602}$ $(U_{0.858}Y_{0.070}Ce_{0.021}Mn_{0.005})_{\Sigma=0.954}$ $(Fe^{3+}{}_{1.695}Zn_{0.305})_{\Sigma=2.000}$ $(Ti_{12.070}Fe^{3+}{}_{4.987}V^{5+}{}_{0.372}Al_{0.030}Nb_{0.030}Cr_{0.015}Sn_{0.001})_{\Sigma=17.505}O_{38}$ (MA).

Mapiquiroite, as well as the other members of the crichtonite group, hosts elements with variable oxidation states. Vanadium and manganese were assumed as V^{5+} and Mn^{2+}, respectively, in agreement with the oxidation states reported for other members of the crichtonite group; however, it should be noted that the specimen from Monte Arsiccio occurs in veins containing stibivanite, $Sb^{3+}{}_2V^{4+}O_5$ and we cannot exclude a 4+ oxidation state for vanadium. As a matter of fact, its low content does not change significantly the results. Cerium was reported as Ce^{3+}, owing to its association, in the specimen from BdV,

Table 1. Reflectance values (%) for mapiquiroite.

	Buca della Vena mine		Monte Arsiccio mine	
λ (nm)	$R_{\min}$	$R_{\max}$	$R_{\min}$	$R_{\max}$
471.1	17.0	17.2	17.7	18.0
548.3	16.7	17.0	17.6	17.8
586.6	16.4	16.7	17.3	17.7
652.3	16.1	16.3	17.0	17.3

Table 2. Electron-microprobe analyses of mapiquiroite.

	Buca della Vena mine		Monte Arsiccio mine	
Oxide	wt%	range	wt%	range
Na_2O	0.05(2)	0.02–0.07	0.03(3)	0.00–0.09
CaO	0.08(2)	0.07–0.12	0.04(10)	0.00–0.39
MnO	0.28(5)	0.23–0.35	0.02(2)	0.00–0.07
ZnO	nd		1.29(6)	1.21–1.38
Al_2O_3	0.09(5)	0.06–0.18	0.08(3)	0.01–0.14
TiO_2	54.14(82)	53.21–55.03	50.14(22)	49.56–50.43
V_2O_5	0.64(8)	0.51–0.72	1.76(22)	1.55–2.67
Cr_2O_3	6.73(110)	6.08–8.63	0.06(6)	0.01–0.23
Fe_2O_3	23.28(102)	21.65–24.25	27.74(45)	27.02–28.64
SrO	3.01(6)	2.93–3.08	1.68(15)	1.36–1.98
Y_2O_3	1.26(11)	1.20–1.46	0.41(9)	0.24–0.53
Nb_2O_5	0.05(5)	0.00–0.11	0.21(11)	0.03–0.48
SnO_2	0.11(5)	0.03–0.14	0.01(1)	0.00–0.04
La_2O_3	1.56(22)	1.28–1.83	0.08(10)	0.00–0.30
Ce_2O_3	0.90(13)	0.68–1.00	0.18(10)	0.00–0.33
PbO	1.28(24)	0.92–1.59	2.88(32)	1.93–3.36
UO_2	5.99(97)	4.40–6.97	12.05(22)	11.75–12.52
Total	99.45		98.66	

with monazite-(Ce) and allanite-(Ce), even if we cannot exclude a 4+ oxidation state, in agreement with the hypothesis of Gatehouse *et al.* (1978, 1979) about the possible occurrence of Ce^{4+} at the M1 site. In addition, according to Săbău & Alberico (2007), crichtonite group minerals from hydrothermal veins contain octahedrally coordinated Ce^{4+}, in agreement with a higher oxidation state indicated by prevalent Fe^{3+}. Tin, never reported in members of the crichtonite group, occurs in negligible amounts and was assumed as Sn^{4+}.

2.3. Crystallography

X-ray powder diffraction patterns collected using a 114.6 mm Gandolfi camera with Ni-filtered Cu $K\alpha$ radiation on unheated grains from BdV gave only few extremely weak diffraction effects. This is a consequence of the partially metamict state of mapiquiroite, related to its significant content of uranium. After thermal treatment (850°C for 24 h), the crystal still gave few very weak reflections, agreeing with those of the members of crichtonite group. Consequently, in Table 3, only the calculated X-ray diffraction patterns are reported.

Unit-cell parameters of the unheated crystals of mapiquiroite are *a* 10.4084(2), *c* 20.9443(5) Å, *V* 1965.01(7) Å^3 (BdV) and *a* 10.4721(3), *c* 21.1412(8) Å, *V* 2007.83(7) Å^3 (MA). The larger cell volume for the more U-rich sample (MA) may be tentatively related to the swelling of the unit cell as a consequence of metamictization, as described for cleusonite (Wülser *et al.*, 2005) and zircon (Murakami *et al.*, 1991; Salje *et al.*, 1999). Notwithstanding the partly metamict nature of mapiquiroite, the X-ray diffraction reflections were sharp and allowed us to collect intensity data. The single-crystal X-ray diffraction study was performed using a Bruker Smart Breeze diffractometer equipped with an air-cooled CCD detector and graphite-monochromatized Mo $K\alpha$ radiation. Intensity data were integrated and corrected for Lorentz, polarization, background effects, and absorption using the package of software APEX2 (Bruker AXS Inc., 2004). The refinements were started using the atom positions of paseroite given by Mills *et al.* (2012) using SHELX-97 (Sheldrick, 2008), and scattering curves for neutral atoms taken from the *International Tables for X-ray Crystallography* (Wilson, 1992). The following curves were used: Pb *vs.* □ for M0 site; U *vs.* □ for M1 site; Fe *vs.* □ for M2 and M3 sites; and Ti *vs.* □ for M4 and M5 sites. The examination of the difference-Fourier maps indicated the occurrence of four additional sites, as reported by previous authors (*e.g.*, Armbruster & Kunz, 1990; Orlandi *et al.*, 1997). The site occupancies of these sites, named M6–M9, were freely refined using the neutral scattering curve of Fe, in agreement with Armbruster & Kunz (1990). After several cycles of refinement, R_1 converged to 0.037 for 1589 observed reflections and 0.084 for 1173 observed reflections for samples from BdV and MA, respectively. Although satisfying *R* indices indicated the correctness of the structural models, the total refined site-scattering values significantly differ from those calculated from electron-microprobe data. This difference (up to ~70 electrons per formula unit for the specimen from MA) is larger with increasing U content and could probably be related to the partly metamict nature of the unheated crystals.

Table 3. Calculated X-ray powder diffraction data for mapiquiroite, obtained using the software POWDER CELL 2.3 (Kraus & Nolze, 1996) on the basis of the structural model obtained through the structure refinements. Only the reflections with $I_{calc} > 10$ are listed. The five strongest reflections are shown in bold.

	Buca della Vena		Monte Arsiccio	
h k l	d_{calc}	I_{calc}	d_{calc}	I_{calc}
1 0 1	8.25	16	8.26	17
1 0 −2	**6.81**	**76**	**6.82**	**86**
1 1 0	**5.18**	**100**	**5.19**	**100**
1 0 4	**4.51**	**44**	**4.52**	**49**
2 0 2	4.125	29	4.131	31
0 0 6	3.479	11	3.482	11
2 0 −4	**3.404**	**41**	**3.408**	**40**
2 1−2, 1 2 2	3.228	17, 13	3.233	18, 15
3 0 0	**2.994**	**35**	**2.998**	**33**
1 1 6, 1 1 −6	2.889	29, 27	2.892	28, 26
2 1 4, 1 2 −4	2.846	27, 11	2.849	26, 13
2 2 0	2.593	20	2.596	20
1 3 −2	2.423	11	2.426	11
1 3 4, 3 1 −4	2.248	11, 15	2.251	14, 12
1 3 10	1.600	10		

The crystals were then annealed at 850°C for 24 h and were used for a new X-ray diffraction study. The room-temperature unit-cell parameters of the heated crystals of mapiquiroite are *a* 10.3719(7), *c* 20.875(1) Å, *V* 1944.8(2) Å^3 (BdV) and *a* 10.3854(3), *c* 20.8942(6) Å, *V* 1951.7(1) Å^3 (MA). The stronger cell-volume contraction of the more U-rich sample (MA) upon annealing is further evidence for partial metamictization of the untreated samples. Intensity data collections were performed as described above, and the structure refinements started using the atomic coordinates found in the refinement of the unheated crystals. The new refinements converged to $R_1 = 0.028$ (BdV) and 0.032 (MA). The total refined site-scattering values are now in quite good agreement with the calculated ones, with differences of +1.5 % and –2.9 % for the specimens from BdV and MA, respectively.

Details of the data collection and crystal-structure refinement for the annealed crystals are reported in Table 4. Atomic coordinates and equivalent isotropic displacement parameters are shown in Table 5, whereas Table 6 reports selected bond distances.

3. Crystal-structure description and crystal chemistry

3.1. General features

As for the other members of the crichtonite group, mapiquiroite crystallizes in the space group $R\bar{3}$ and its crystal

Table 4. Crystal data and summary of parameters describing data collections and refinements for annealed crystals of mapiquiroite.

	Buca della Vena mine	Monte Arsiccio mine
Crystal data		
Crystal size (mm^3)	0.20 × 0.06 × 0.05	0.14 × 0.06 × 0.02
Cell setting, space group	Trigonal, $R\overline{3}$	
a, c (Å);	10.3719(7), 20.8752(4)	10.3854(3), 20.8942(6)
V (Å^3)	1944.8(2)	1951.65(10)
Z	3	
Data collection and refinement		
Radiation, wavelength	Mo $K\alpha$, $\lambda = 0.71073$Å	
Temperature (K)	293	
$2\theta_{max}$ (°)	73.73	67.16
Measured reflections	6478	6948
Unique reflections	2071	1629
Reflections with $F_o > 4\sigma(F_o)$	1815	1347
R_{int}	0.0227	0.0365
$R\sigma$	0.0255	0.0378
Range of h, k, l	$-17 \leq h \leq 13$, $-11 \leq k \leq 17$, $-33 \leq l \leq 32$	$-16 \leq h \leq 13$, $-15 \leq k \leq 15$, $-31 \leq l \leq 29$
R [$F_o > 4\sigma(F_o)$]	0.0281	0.0323
R (all data)	0.0363	0.0495
wR (on F_o^2)	0.0691	0.0749
Goof	1.124	1.120
Number of least-squares parameters	132	132
Maximum and minimum residual peak (e Å^{-3})	1.73 (at 0.70 Å from M1) −0.75 (at 1.18 Å from M5)	1.74 (at 0.69 Å from M1) −1.47 (at 1.06 Å from M6)

structure is defined by layers of close-packed octahedra (M1, M3, M4, M5) and tetrahedra (M2), containing large 12-coordinated M0 sites (Fig. 3).

Crystal-structure refinement highlighted the occurrence of four additional octahedral sites, having low site occupancies. The occurrence of additional sites was first observed by Gatehouse *et al*. (1983) who described the presence of an M6 site in mathiasite. Additional sites were then found by Armbruster & Kunz (1990) in a uranium-rich senaite and by Orlandi *et al*. (1997) in dessauite-(Y). The additional sites observed in mapiquiroite are the same as those occurring in dessauite-(Y), that is three octahedral sites (M6–M8) and one square pyramidal site (M9). Orlandi *et al*. (1997) proposed that the cation disorder over additional sites may be related to the heating process used to improve the crystallinity of dessauite-(Y). Our study, performed collecting intensity data on both unheated and heated crystals, does not confirm the hypothesis, showing the occurrence of the additional sites in the unheated crystals too.

3.2. Cation coordination and site occupancies

The crystal structures of the members of the crichtonite group have usually six main cation sites. As reported above, additional sites with low occupancies can be present. The chemical composition can be represented by the general formula $^{XII}A^{VI}B^{IV}T_2{}^{VI}C_{18}O_{38}$, where the Roman number preceding each component indicates the coordination number of the site. The cation sites are distributed as follows: A = M0; B = M1; T = M2; C = M3–M5. Site occupancies for the two occurrences of mapiquiroite were hypothesized on the basis of average bond distances and site scattering values, comparing the results of the crystal-structure refinements with the electron microprobe data (Table 7).

The A cations occupy the 12-fold coordinated M0 site. In mapiquiroite this position hosts Sr and Pb, with a (Sr/Pb) atomic ratio of 5.1 and 1.25 for the specimens from BdV

Table 5. Atomic coordinates and equivalent displacement parameters (Å^2) for mapiquiroite.

		Buca della Vena mine				Monte Arsiccio mine			
Site	Wyckoff site	x	y	z	U_{eq}	x	y	z	U_{eq}
M0	3*a*	0	0	0	0.0218(2)	0	0	0	0.0252(3)
M1	3*b*	0	0	½	0.0071(1)	0	0	½	0.0060(1)
M2	6*c*	0	0	0.30924(3)	0.0070(2)	0	0	0.30916(4)	0.0060(3)
M3	18*f*	0.18354(4)	0.03965(4)	0.16506(2)	0.0075(1)	0.18392(7)	0.03759(7)	0.16506(3)	0.0088(2)
M4	18*f*	0.08388(4)	0.33058(5)	0.60827(2)	0.0101(1)	0.08290(8)	0.33044(8)	0.60845(3)	0.0091(2)
M5	18*f*	0.07587(4)	0.31937(4)	0.39877(2)	0.0089(1)	0.07605(8)	0.32015(8)	0.39863(3)	0.0081(2)
M6	18*f*	0.7689(5)	0.0766(5)	0.4999(2)	0.0021(13)	0.7682(9)	0.0771(9)	0.5000(3)	0.024(3)
M7	18*f*	0.1807(10)	0.0512(10)	0.2725(4)	0.012(3)	0.1795(18)	0.0519(18)	0.2724(6)	0.025(5)
M8	6*c*	0	0	0.3905(8)	0.031(5)	0	0	0.3921(11)	0.020(8)
M9	18*f*	0.5376(10)	0.1544(10)	0.3945(4)	0.014(3)	0.5398(18)	0.1539(18)	0.3934(7)	0.037(5)
O1	18*f*	0.1330(2)	0.1904(2)	0.56244(8)	0.0112(3)	0.1314(3)	0.1878(3)	0.5619(1)	0.0111(6)
O2	18*f*	0.7106(2)	0.2060(2)	0.44345(8)	0.0102(3)	0.7111(3)	0.2059(3)	0.4436(1)	0.0106(6)
O3	18*f*	0.3596(2)	0.1013(2)	0.55931(8)	0.0089(3)	0.3594(3)	0.1017(3)	0.5594(1)	0.0094(6)
O4	18*f*	0.5918(2)	0.0321(2)	0.55013(8)	0.0098(3)	0.5917(3)	0.0318(3)	0.5500(1)	0.0108(6)
O5	18*f*	0.0519(2)	0.8560(2)	0.33592(7)	0.0094(3)	0.0511(3)	0.8569(3)	0.3355(1)	0.0078(6)
O6	18*f*	0.3666(2)	0.0990(2)	0.33985(8)	0.0094(3)	0.3654(3)	0.0985(3)	0.3397(1)	0.0086(6)
O7	6*c*	0	0	0.2155(1)	0.0095(5)	0	0	0.2163(2)	0.0072(9)

Table 6. Selected *Me*–S bond distances (in Å) in mapiquiroite.

		Buca della Vena mine	Monte Arsiccio mine
M0	– O2	2.799(2) × 6	2.809(3) × 6
	– O6	2.837(2) × 6	2.850(3) × 6
	average	2.818	2.830
M1	– O1	2.186(2) × 6	2.163(3) × 6
M2	– O5	1.906(2) × 3	1.893(3) × 3
	– O7	1.958(3)	1.941(4)
	average	1.919	1.905
M3	– O4	1.938(2)	1.931(3)
	– O3	1.971(2)	1.959(3)
	– O2	1.976(2)	1.965(3)
	– O4	2.011(2)	2.027(3)
	– O7	2.029(2)	2.049(2)
	– O2	2.077(2)	2.101(3)
	average	2.000	2.005
M4	– O2	1.878(2)	1.884(3)
	– O6	1.944(2)	1.940(3)
	– O3	1.964(2)	1.961(3)
	– O1	2.007(2)	2.034(3)
	– O6	2.057(2)	2.065(3)
	– O5	2.088(2)	2.094(3)
	average	1.990	1.996
M5	– O4	1.867(2)	1.868(3)
	– O1	1.906(2)	1.929(3)
	– O3	1.931(2)	1.930(3)
	– O5	2.005(2)	2.005(3)
	– O6	2.029(2)	2.027(3)
	– O5	2.183(2)	2.201(3)
	average	1.987	1.993
M6	– O4	1.959(4)	1.952(8)
	– O1	2.056(4)	2.068(8)
	– O3	2.062(4)	2.070(8)
	– O3	2.089(4)	2.086(8)
	– O2	2.095(4)	2.078(8)
	– O1	2.098(4)	2.107(8)
	average	2.060	2.060
M7	– O3	1.907(9)	1.92(2)
	– O4	1.986(9)	1.99(2)
	– O7	2.053(9)	2.03(2)
	– O5	2.173(9)	2.15(2)
	– O5	2.221(9)	2.22(2)
	– O6	2.233(9)	2.24(2)
	average	2.096	2.09
M8	– O1	2.011(8) × 3	1.98(1) × 3
	– O5	2.150(9) × 3	2.16(1) × 3
	average	2.080	2.07
M9	– O2	1.895(9)	1.90(2)
	– O6	1.938(9)	1.96(1)
	– O2	1.952(9)	1.98(2)
	– O4	2.069(9)	2.08(2)
	– O6	2.197(9)	2.17(2)
	average	2.010	2.02

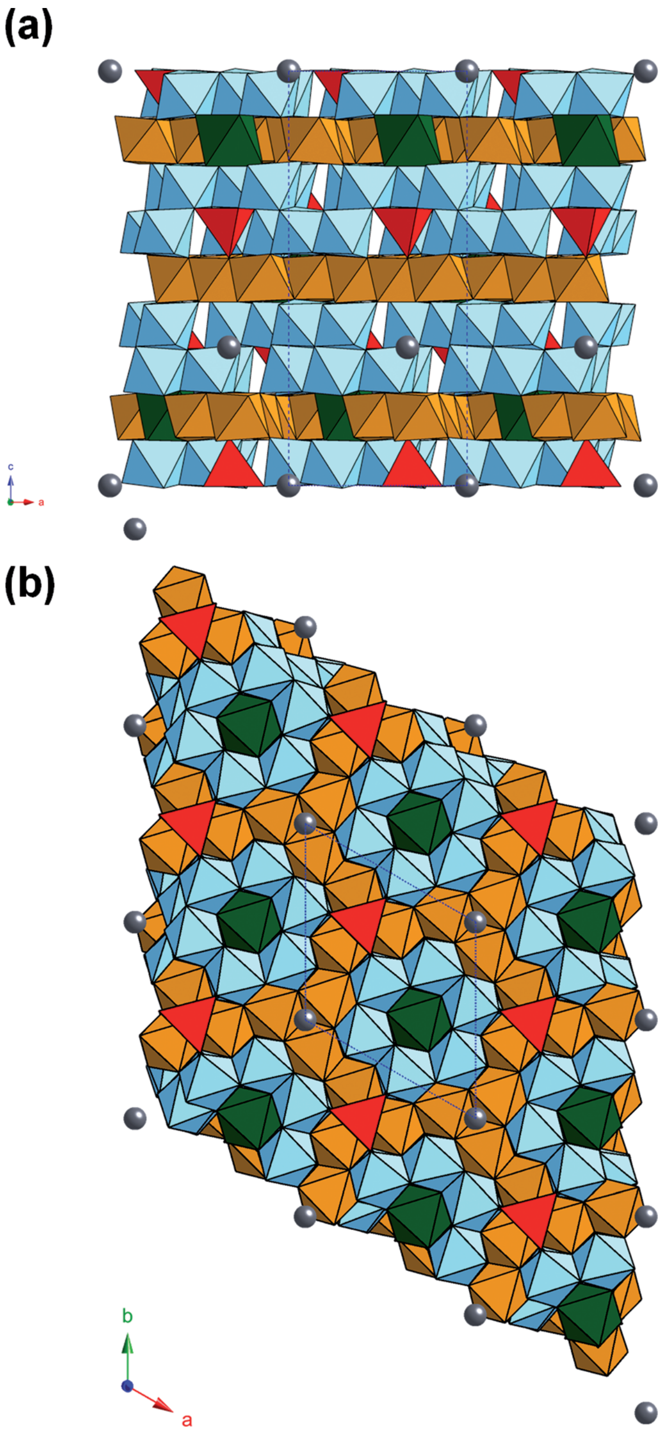

Fig. 3. The layered crystal structure of mapiquiroite as seen down **b** (**c** vertical, **a** horizontal) and **c** (**b** vertical). Grey spheres: M0 site. Polyhedra: dark green, M1; red, M2; orange, M3; light blue, M4 and M5. (colours in the electronic version of the paper). (online version in colour)

and MA, respectively. The average <M0–O> distance is 2.818 and 2.830 Å, in agreement with those reported for other members of the crichtonite group (Table 8). Whereas the <M0–O> bond distance for mapiquiroite from BdV is in good agreement with those observed in other phases having mixed (Pb,Sr) or (Sr,Pb) site occupancies at M0 (*e.g.*, dessauite-(Y)–Orlandi *et al.*, 1997; gramaccioliite-(Y)–Orlandi *et al.*, 2004b), the average bond distance for M0 site for the specimen from MA is slightly longer, possibly indicating the occurrence of minor amounts of large cations (*e.g.*, Ba). Strontium and lead are partially substituted by minor La, Na, and Ca. The agreement between observed and calculated site scattering at M0 in the specimen from BdV can be considered as satisfying; on the other hand, a significant difference is observed for the

Table 7. Refined site scattering values (*epfu*) and assigned site population (*apfu*) for cation sites in mapiquiroite.

Site		EPMA	XRD
Buca della Vena mine			
M0	$\mathrm{Sr}_{0.533}\mathrm{La}_{0.176}\mathrm{Pb}_{0.105}\mathrm{Na}_{0.030}\mathrm{Ca}_{0.026}\square_{0.130}$	39.7	35.7
M1	$\mathrm{U}_{0.407}\mathrm{Ce}_{0.101}\mathrm{Y}_{0.205}\mathrm{Mn}_{0.072}\square_{0.215}$	53.2	57.2
M2	$\mathrm{Fe}^{3+}_{2.000}$	52.0	40.7
M3 + M4 + M5	$\mathrm{Ti}_{12.423}\mathrm{Fe}^{3+}_{3.345}\mathrm{Cr}^{3+}_{1.624}\mathrm{V}^{5+}_{0.129}\mathrm{Al}_{0.032}\mathrm{Sn}_{0.013}\mathrm{Nb}_{0.007}\square_{0.427}$	403.6	386.5
M6			9.4
M7			5.8
M8			2.9
M9			2.0
		$\Sigma = 548.5$	540.2
Monte Arsiccio mine			
M0	$\mathrm{Sr}_{0.312}\mathrm{Pb}_{0.248}\mathrm{Na}_{0.019}\mathrm{Ca}_{0.014}\mathrm{La}_{0.009}\square_{0.398}$	33.2	44.6
M1	$\mathrm{U}_{0.858}\mathrm{Y}_{0.070}\mathrm{Ce}_{0.021}\mathrm{Mn}_{0.005}\square_{0.046}$	83.0	73.0
M2	$\mathrm{Fe}^{3+}_{1.695}\mathrm{Zn}_{0.305}$	52.6	46.8
M3 + M4 + M5	$\mathrm{Ti}_{12.070}\mathrm{Fe}^{3+}_{4.987}\mathrm{V}^{5+}_{0.372}\mathrm{Al}_{0.030}\mathrm{Nb}_{0.030}\mathrm{Cr}_{0.015}\mathrm{Sn}_{0.001}\square_{0.495}$	405.8	402.0
M6			14.7
M7			2.6
M8			2.4
M9			9.3
		$\Sigma = 578.2$	595.4

Table 8. Average bond distances (in Å) for the different cation sites in members of the crichtonite group.

		M0	M1	M2	M3	M4	M5	References
Cleusonite			no structural data available					Wülser *et al.* (2005)
Crichtonite		2.792	2.205	1.972	2.006	1.969	1.967	Grey *et al.* (1976)
‘‘Davidite’’		2.769	2.243	1.981	2.010	1.975	1.972	Gatehouse *et al.* (1979)
Dessauite-(Y)		2.814	2.194	1.938	2.011	1.990	1.983	Orlandi *et al.* (1997)
Gramaccioliite-(Y)		2.813	2.225	1.957	2.015	1.967	1.980	Orlandi *et al.* (2004b)
Landauite		2.822	2.211	1.963	1.997	1.973	1.969	Grey & Gatehouse (1978)
Lindsleyite		2.837	2.119	1.948	1.982	1.990	1.978	Zhang *et al.* (1988)
Loveringite		2.789	2.166	1.994	1.983	1.971	1.970	Gatehouse *et al.* (1978)
Mapiquiroite	BdV	2.818	2.186	1.919	2.000	1.990	1.987	this work
	MA	2.830	2.163	1.905	2.005	1.996	1.993	this work
Mathiasite		2.832	2.132	1.981	1.980	1.978	1.971	Gatehouse *et al.* (1983)
Paseroite		2.856	2.131	1.959	1.973	2.014	1.990	Mills *et al.* (2012)
Senaite		2.817	2.227	1.996	1.998	1.976	1.964	Grey & Lloyd (1976)
U-rich senaite		2.873	2.167	1.948	2.016	2.010	1.997	Armbruster & Kunz (1990)

specimen from MA. However, it is noteworthy that the site scattering excess at the M0 site corresponds to a deficit at the M1 site and a possible different cation distribution could be hypothesized.

The *B* cations, hosted at the M1 site, are represented by small cations. Average <M1–O> bond distances decrease with the increase of U content, passing from 2.186 Å (BdV) to 2.163 Å (MA). The latter bond distance is in good agreement with the value (2.167 Å) observed by Armbruster & Kunz (1990) for U-rich senaite. In the specimen from BdV, Ce was introduced at the M1 site in order to achieve a better fit between the observed and calculated site scattering. If our assumption is correct, it is probable that Ce occurs as Ce^{4+} whose ionic radius, 0.87 Å (Shannon, 1976), is similar to that of U^{4+} and Y^{3+}.

The *C* cations, at the M3, M4, and M5 sites, are mainly represented by Ti and Fe^{3+}, with minor substitutions by Cr and V in the specimens from BdV and MA, respectively. The average bond distances for these sites agree with data reported by previous authors for other members of the crichtonite group (Table 8).

On the contrary, the M2 site, hosting *T* cations, has a significantly shorter average bond distance, the shortest reported so far in this group of oxides. The only other mineral phase having a similar <M2–O> bond distance is dessauite-(Y). Such a feature could be related to the oxidized nature of iron, preferentially occurring as Fe^{3+}. The possible substitution of Fe^{2+} by Fe^{3+} at the M2 site was first hypothesized by Grey *et al.* (1976), who observed a slightly shorter <M2–O> distance in crichtonite with respect to that observed in senaite (Grey & Lloyd, 1976). The oxidation state of Fe in crichtonite will be discussed in the following paragraph.

3.3. Oxidation states of iron and uranium

The crystal structure of the members of the crichtonite group can host a large number of cations displaying different oxidation states. Among these cations, the most important is certainly iron, which can occur as Fe^{2+} and/or Fe^{3+}. As outlined by Wülser *et al.* (2005), the Fe^{2+}/Fe^{3+} ratio cannot be confidently calculated from electron-microprobe analysis; as a consequence independent measurements (*e.g.*, Mössbauer spectroscopy, X-ray photoelectron spectroscopy) have to be performed. However, even if the largest crystal of mapiquiroite observed during this study would be large enough for such analyses being carried out, only a few fragments were available to us for this study, owing to the extreme rarity of mapiquiroite at both localities. Consequently, some speculations about the oxidation states of iron were made based upon the observed bond distances only.

Ionic radii of four-fold coordinated Fe^{2+} and Fe^{3+} are 0.63 and 0.49 Å (Shannon, 1976), respectively. Oxygen atoms coordinating iron hosted at M2 are four-fold coordinated, and their ionic radius is 1.38 Å. Consequently, the average bond distance $<Fe^{2+}–O>$ and $<Fe^{3+}–O>$ should be 2.01 and 1.87 Å, respectively. In the specimen from BdV, M2 is occupied by Fe only, whereas Fe and Zn occur at the M2 site (ideal occupancy $Fe_{0.85}Zn_{0.15}$) of the sample from MA. The ionic radius of four-fold coordinated Zn^{2+} is 0.60 Å, and the ideal bond distance for the specimen from MA should be 2.01 Å (if Fe is assumed to be divalent) and 1.89 Å if Fe occurs as Fe^{3+}. The latter value agrees with the observed one (1.905 Å). Consequently, structural data seem to indicate that M2 is mainly occupied by Fe^{3+}, instead of Fe^{2+} as reported for other members of the crichtonite group. In the specimen from BdV, the average bond distance could indicate the occurrence of Fe^{3+} and minor Fe^{2+} at the M2 site, in the ratio 65:35.

One can hypothesize that the oxidation of Fe is a consequence of the heating process in air. Actually, our results indicate that it is a pristine feature. In fact, the average <M2–O> bond distances observed for the unheated crystals are 1.931 (BdV) and 1.901 Å (MA). The average <M2–O> distance in the crystal from BdV decreases of 0.012 Å. If we assume a mixed (Fe^{3+},Fe^{2+}) occupancy, the site occupancy can be written as ($Fe^{3+}_{0.56}Fe^{2+}_{0.44}$) in the unheated fragment and ($Fe^{3+}_{0.65}Fe^{2+}_{0.35}$) in the heated fragment. The difference could be negligible and oxidation of Fe^{2+} to Fe^{3+} could not occur. In the sample from MA, on the contrary, we observed a very small increase of the average <M2–O> distance, from 1.901 Å in the unheated fragment to 1.905 Å in the heated fragment.

In addition to iron, uranium is another element displaying variable oxidation states. Wülser *et al.* (2005) reported U^{4+} and U^{6+} in cleusonite. Taking into account that the redox potential of the pair Fe^{3+}/Fe^{2+} is considerably higher than that of the U^{6+}/U^{4+} pair, if all Fe is trivalent, it is likely that all U is hexavalent; conversely, if any U is tetravalent, it is likely that all Fe is divalent. Actually, through XPS spectroscopy, Wülser *et al.* (2005) found the coexistence of Fe^{2+}, Fe^{3+}, U^{4+}, and U^{6+} in cleusonite, with a ratio 71:29 for the pair Fe^{2+}/Fe^{3+} and 72:28 for the pair U^{4+}/U^{6+}. No direct measurements were performed on mapiquiroite and, as discussed for the iron oxidation state, we can only speculate on the basis of bond distances. Uranium is hosted at the M1 site and is partially substituted by Y. Ionic radii of six-fold coordinated U^{6+}, U^{4+}, and Y^{3+} are 0.73, 0.89, and 0.90 Å, respectively (Shannon, 1976). The M1 site is coordinated by O1, that is in three-fold coordination. Consequently, in agreement with Shannon (1976), its ionic radius is 1.36 Å. Therefore, the ideal $<U^{6+}–O>$, $<U^{4+}–O>$, and <Y–O> bond distances should be 2.09, 2.25, and 2.26 Å, respectively. The ionic radii of U^{4+} and Y are very similar, and consequently the observed average bond distances (2.186 and 2.163 Å for BdV and MA, respectively) would be attributed to the substitution of (U^{4+},Y) by a smaller cation. The only possible substitution is the occurrence of minor Ce^{4+} (if any) at the M1 site of mapiquiroite from MA; however, its ionic radius (0.87 Å) is similar to that of U^{4+} and Y and does not explain the contraction of the site. Moreover, in the specimen from MA, the M1 site can be considered a pure U site. Consequently, we hypothesize that the average bond distances observed for the M1 site agree with a partial substitution of U^{4+} and Y by the smaller U^{6+}.

4. Discussion

4.1. Chemical variability in mapiquiroite

According to Wülser *et al.* (2004), the complex chemical composition of the members of the crichtonite group is in a strict relationship with the geological environment of crystallization and it seems to be controlled by several factors. In particular, the host-rock trace-elements signature (*e.g.*, Cr, V, Mn) may be reflected in the composition of the minerals of the crichtonite group. Consequently, the chemical variability between the two occurrences of mapiquiroite can be related to the different geochemistry of the host-rocks.

The most striking difference between the two occurrences of mapiquiroite is definitely the chromium content. In fact, the Cr content of mapiquiroite from BdV is exceptionally high; only loveringite (~10 wt% Cr_2O_3; Gatehouse *et al.*, 1978), lindsleyite and mathiasite (up to 18 wt% Cr_2O_3; Haggerty *et al.*, 1983) have a higher chromium content. On the contrary, mapiquiroite from MA has a negligible content of this element. It is noteworthy that dessauite-(Y), described by Orlandi *et al.* (1997) from

BdV, has a very low content of Cr_2O_3 (0.21 wt%). The different chromium content of these two members of the crichtonite group coming from the same locality is probably related to the different occurrence, that is quartz + 'adularia' + baryte veins embedded in schists and calcite veins embedded in dolostones for mapiquiroite and dessauite-(Y), respectively. The schists embedding the quartz + 'adularia' + baryte veins at BdV host a Cr-rich mica, characterized by an emerald-green colour.

Whereas Cr is the main substituent of Ti and Fe at the M3–M5 sites in the crystal structure of mapiquiroite from BdV, vanadium plays the same role in the specimen from MA. Indeed, its abundance reaches only 0.37 apfu. The higher vanadium content of the sample from MA with respect to that from BdV agrees with the occurrence of stibivanite in the veins embedded in magnetite-rich dolostone, at a short distance (few centimetres) from the quartz–carbonate veins in which mapiquiroite was found. Dessauite-(Y) has an intermediate V content, *i.e.* 0.19 apfu (Orlandi *et al.*, 1997).

Uranium is an unusual element in the hydrothermal veins from Apuan Alps and only few uranium mineral species have been reported so far (*e.g.*, uraninite from the Carrara marble cavities; Orlandi & Del Chiaro, 1989). The U content varies from 12.05 wt% UO_2 in the specimen from MA down to 5.99 wt% in the specimen from BdV. Dessauite-(Y) has an average UO_2 content of 4.52 wt%, ranging from 2.63 to 8.74 wt%. Whereas the U content of the specimen from MA does not vary significantly, ranging from 11.75 to 12.52 wt%, the UO_2 content in the specimen from BdV vary between 4.40 and 6.97 wt%. Taking into account the wide range of UO_2 content reported by Orlandi *et al.* (1997) for dessauite-(Y), we could infer that this species and mapiquiroite can occur closely associated, as a consequence of the possible existence of a solid solution between these two phases.

Taking into account the Sr and Pb content, the specimen from BdV is definitely Sr-dominant, whereas mapiquiroite from MA has a composition near the boundary with cleusonite. In fact, one spot analysis collected on the sample from this latter locality corresponds to a Sr-rich cleusonite (Fig. 4).

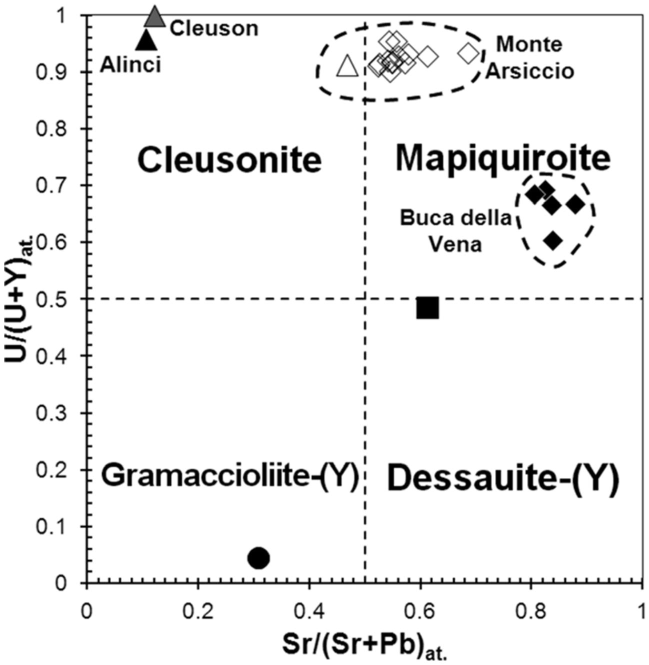

Fig. 4. Chemical variability in members of the crichtonite group with M0 = Sr or Pb and M1 = Y or U. Data are from Bermanec *et al.* (1992), Orlandi *et al.* (1997, 2004b) and Wülser *et al.* (2005).

4.2. Yttrium and uranium members of the crichtonite group

Owing to their complex crystal chemistry, thirteen different mineral species belonging to the crichtonite group are known; Table 9 reports their idealized site occupancies. Wülser *et al.* (2004) proposed a classification of the members of the crichtonite group based upon their genesis. They distinguished magmatic *versus* metamorphic subgroups.

Table 9. Mineral species related to mapiquiroite and idealized site occupancies.

	M0	M1	M2	M3–5	References
Cleusonite	Pb,Sr	U	Fe,Zn	Ti,Fe	Wülser *et al.* (2005)
Crichtonite	Sr,Ba,Pb	Mn	Fe,Zn	Ti,Fe	Grey *et al.* (1976)
Davidite-(Ce)	Ce,La	Y,HREE,U	Fe,Mg	Ti,Fe,Cr,V	Gatehouse *et al.* (1979)
Davidite-(La)	La,Ce	Y,HREE,U	Fe,Mg	Ti,Fe,Cr,V	Gatehouse *et al.* (1979)
Dessauite-(Y)	Sr,Pb	Y,U	Fe,Zn	Ti,Fe	Orlandi *et al.* (1997)
Gramaccioliite-(Y)	Pb,Sr	Y,Mn	Fe,Zn	Ti,Fe	Orlandi *et al.* (2004b)
Landauite	Na,Pb	Mn,Y	Zn	Ti,Fe,Nb	Grey & Gatehouse (1978)
Lindsleyite	Ba,K	Zr,Fe	Mg,Fe	Ti,Cr,Fe	Zhang *et al.* (1988)
Loveringite	Ca,LREE	Zr,Fe	Mg,Fe	Ti,Fe,Cr,Al	Gatehouse *et al.* (1978)
Mapiquiroite	Sr,Pb	U,Y	Fe	Ti,Fe	this work
Mathiasite	K,Ba,Sr	Zr,Fe	Mg,Fe	Ti,Cr,Fe	Gatehouse *et al.* (1983)
Paseroite	Pb,Sr	Mn	Fe,Zn	V,Ti,Fe	Mills *et al.* (2012)
Senaite	Pb,Sr	Mn	Fe,Zn	Ti,Fe	Grey & Lloyd (1976)

Mapiquiroite belongs to the metamorphic crichtonites; according to Wülser *et al.* (2004), five valid mineral species and an unnamed mineral form this sub-group (senaite subgroup in their classification). Mapiquiroite corresponds to the unnamed mineral of these authors. Taking into account the occupancy of M0, we can distinguish Pb-dominant phases and Sr-dominant phases. Then, considering the occupancy at the M1 site, three different minerals in each group occur, having Mn, Y, and U as dominant cation at this site.

Considering only the members rich in uranium and yttrium, we have four mineral phases: cleusonite, gramaccioliite-(Y), mapiquiroite, and dessauite-(Y). Wülser *et al.* (2005) reviewed the occurrences of cleusonite, considering the previous description of U-bearing crichtonites. Several names were used to describe uraniferous terms of the crichtonite group: 'plumbodavidite' (Wang, 1981), 'miromirite' (Vujanovic, 1969; Fleischer, 1973), and 'romanite' (Dragila, 1990; Jambor & Puziewicz, 1992). The review of Wülser *et al.* (2005) allowed them to ascertain that 'plumbodavidite' corresponds to cleusonite, whereas the other two minerals were not sufficiently characterized to allow a clear identification. In addition, the specimen of U-rich senaite described by Bermanec *et al.* (1992) from Alinci, Macedonia, corresponds to cleusonite. There are some other descriptions of minerals belonging to the crichtonite group showing, for example, intermediate compositions between cleusonite and davidite-(Ce) (Mossman, 1985), in agreement with the solution between members of the senaite sub-group and those belonging to the davidite subgroup, as defined by Wülser *et al.* (2004).

The description of mapiquiroite is not only a further demonstration of the extraordinary geochemical variability of the baryte + pyrite + iron oxide ore deposits from the Apuan Alps, but it fills an important gap in the nomenclature of uranium-containing members of the crichtonite group.

Acknowledgements: Electron microprobe analyses were performed with the kind assistance of Raul Carampin. We are grateful to the mineral collectors Luigi Pierotti, Ugo Quilici, and Moreno Romani for providing us with the first specimens of mapiquiroite. Italo Campostrini is thanked for the SEM image of mapiquiroite from Buca della Vena mine. Finally, Noah Hobbs is warmly thanked for the photograph of the southern part of the Buca della Vena mine. The paper was handled by Sergey V. Krivovichev and benefited from the comments of two anonymous reviewers.

References

Armbruster, T. & Kunz, M. (1990): Cation arrangement in an unusual uranium-rich senaite: crystal structure study at 130 K. *Eur. J. Mineral.*, **2**, 163–170.

Benvenuti, M., Lattanzi, P., Tanelli, G., Cortecci, G. (1986): The Ba-Fe-pyrite deposit of Buca della Vena mine, Apuan Alps, Italy. *Rend. Soc. Ital. Mineral. Petrol.*, **41**, 347–358.

Bermanec, V., Tibjaš, D., Kniewald, G. (1992): Uranium-rich metamict senaite from Alinci, Yugoslavia. *Eur. J. Mineral.*, **4**, 331–335.

Biagioni, C. & Orlandi, P. (2010): Cymrite and benstonite from the Monte Arsiccio mine (Apuan Alps, Tuscany, Italy): first Italian occurrence. 89th SIMP Meeting, Book of Abstracts, Ferrara, 13rd–15th September 2010.

Biagioni, C., Orlandi, P., Pasero, M. (2009): Ankangite from the Monte Arsiccio mine (Apuan Alps, Tuscany, Italy): occurrence, crystal structure, and classification problems in cryptomelane group minerals. *Per. Mineral.*, **78**, 3–11.

Biagioni, C., Bonaccorsi, E., Moëlo, Y., Orlandi, P. (2013a): Mercury-arsenic sulfosalts from Apuan Alps (Tuscany, Italy). I. Routhierite, $(Cu_{0.8}Ag_{0.2})Hg_2Tl(As_{1.4}Sb_{0.6})_{\Sigma=2}S_6$, from Monte Arsiccio mine: occurrence and crystal structure. *Eur. J. Mineral.*, DOI: 10.1127/0935-1221/2013/0025-2320

Biagioni, C., D'Orazio, M., Vezzoni, S., Dini, A., Orlandi, P. (2013b): Mobilization of Tl-Hg-As-Sb-(Ag,Cu)-Pb sulfosalt melts during low-grade metamorphism in the Alpi Apuane. *Geology*, **41**, 747–750.

Biagioni, C., Orlandi, P., Nestola, F., Bianchin, S. (2013c): Oxycalcioroméite, $Ca_2Sb_2O_6O$, from Buca della Vena mine, Apuan Alps, Tuscany, Italy: a new member of the pyrochlore supergroup. *Mineral. Mag.*, **77**, 3027–3037.

Biagioni, C., Bonaccorsi, E., Moëlo, Y., Orlandi, P., Bindi, L., D'Orazio, M., Vezzoni, S. (2014): Mercury-arsenic sulfosalts from the Apuan Alps (Tuscany, Italy). II. Arsiccioite, $AgHg_2TlAs_2S_6$, a new mineral from the Monte Arsiccio mine: occurrence, crystal structure and crystal chemistry of the routhierite isotypic series. *Mineral. Mag.*, **78**, 101–117.

Bruker AXS Inc (2004): APEX 2. *Bruker Advanced X-ray Solutions*. Madison, Wisconsin.

Costagliola, P., Benvenuti, M., Tanelli, G., Cortecci, G., Lattanzi, P. (1990): The barite-pyrite-iron oxides deposit of Monte Arsiccio (Apuane Alps). Geological setting, mineralogy, fluid inclusions, stable isotopes and genesis. *Boll. Soc. Geol. It.*, **109**, 267–277.

Dragila, M. (1990): Observatli mineralogice asupra unul nou mineral din grupa daviditulul. *Revista Minelor/Mine Petrol Si Gaze*, **41**, 414–418.

Fleischer, M. (1973): New mineral names. *Am. Mineral.*, **58**, 560–562.

Gatehouse, B.M., Grey, I.E., Campbell, I.H., Kelly, P.R. (1978): The crystal structure of loveringite – a new member of the crichtonite group. *Am. Mineral.*, **63**, 28–36.

Gatehouse, B.M., Grey, I.E., Kelly, P.R. (1979): The crystal structure of davidite. *Am. Mineral.*, **64**, 1010–1017.

Gatehouse, B.M., Grey, I.E., Smith, J.R. (1983): Structure refinement of mathiasite $(K_{0.62}Na_{0.14}Ba_{0.14}Sr_{0.10})_{\Sigma1.0}[Ti_{12.90}Cr_{3.10}Mg_{1.53}Fe_{2.15}Zr_{0.67}Ca_{0.29}(V,Nb,Al)_{0.36}]_{\Sigma21}O_{38}$. *Acta Crystallogr.*, **C39**, 421–422.

Grey, I.A. & Gatehouse, B.M. (1978): The crystal structure of landauite, $Na[MnZn_2(Ti,Fe)_6Ti_{12}]O_{38}$. *Can. Mineral.*, **16**, 63–68.

Grey, I.A. & Lloyd, D.J. (1976): The crystal structure of senaite. *Acta Crystallogr.*, **B32**, 1509–1513.

Grey, I.A., Lloyd, D.J., White, Jr. J.S. (1976): The structure of crichtonite and its relationship to senaite. *Am. Mineral.*, **61**, 1203–1212.

Haggerty, S.E., Smyth, J.R., Erlank, A.J., Rickard, R.S., Danchin, R.V. (1983): Lindsleyite (Ba) and mathiasite (K): two new chromium-titanates in the crichtonite series from the upper mantle. *Am. Mineral.*, **68**, 494–505.

Jambor, J.L. & Puziewicz, J. (1992): New mineral names. *Am. Mineral.*, **77**, 1116–1121.

Kraus, W. & Nolze, G. (1996): POWDER CELL – a program for the representation and manipulation of crystal structures and calculation of the resulting X-ray powder patterns. *J. Appl. Crystallogr.*, **29**, 301–303.

Mills, S.J., Bindi, L., Cadoni, M., Kampf, A.R., Ciriotti, M.E., Ferraris, G. (2012): Paseroite, $PbMn^{2+}(Mn^{2+},Fe^{2+})_2(V^{5+},Ti,Fe^{3+},\square)_{18}O_{38}$, a new member of the crichtonite group. *Eur. J. Mineral.*, **24**, 1061–1067.

Mossman, D.J. (1985): Davidite: a review of Canadian occurrences, and report on a recent find at Kommes Lake, Saskatchewan. *Can. Mineral.*, **23**, 495–500.

Murakami, T., Chakoumakos, B.C., Ewing, R.C., Lumpkin, G.R., Weber, W.J. (1991): Alpha-decay event damage in zircon. *Am. Mineral.*, **76**, 1510–1532.

Orlandi, P. & Del Chiaro, L. (1989): Nuovi dati sui minerali delle geodi del marmo di Carrara. *Atti Soc. Tosc. Sci. Nat. Mem.*, **96**, 313–325.

Orlandi, P., Pasero, M., Duchi, G., Olmi, F. (1997): Dessauite, $(Sr,Pb)(Y,U)(Ti,Fe^{3+})_{20}O_{38}$, a new mineral of the crichtonite group from Buca della Vena mine, Tuscany, Italy. *Am. Mineral.*, **82**, 807–811.

Orlandi, P., Dini, A., Olmi, F. (1998): Grumiplucite, a new mercury-bismuth sulfosalt species from the Levigliani mine, Apuan Alps, Tuscany, Italy. *Can. Mineral.*, **36**, 1321–1326.

Orlandi, P., Moëlo, Y., Meerschaut, A., Palvadeau, P., Léone, P. (2004a): Lead-antimony sulfosalts from Tuscany (Italy). VI. Pellouxite, $\sim (Cu,Ag)_2Pb_{21}Sb_{23}S_{55}ClO$, a new oxy-chloro-sulfosalt, from Buca della Vena mine, Apuan Alps. *Eur. J. Mineral.*, **16**, 839–844.

Orlandi, P., Pasero, M., Rotiroti, N., Olmi, F., Demartin, F., Moëlo, Y. (2004b): Gramaccioliite-(Y), a new mineral of the crichtonite group from Stura Valley, Piedmont, Italy. *Eur. J. Mineral.*, **16**, 171–175.

Orlandi, P., Moëlo, Y., Meerschaut, A., Palvadeau, P., Léone, P. (2005): Lead-antimony sulfosalts from Tuscany (Italy): VIII. Rouxelite, $Cu_2HgPb_{22}Sb_{28}S_{64}(O,S)_2$, a new sulfosalt from Buca della Vena mine, Apuan Alps: definition and crystal structure. *Can. Mineral.*, **43**, 919–933.

Orlandi, P., Biagioni, C., Bonaccorsi, E., Moëlo, Y., Paar, W. (2012): Lead-antimony sulfosalts from Tuscany (Italy). XII. Boscardinite, $TlPb_4(Sb_7As_2)_{\Sigma 9}S_{18}$, a new mineral species from Monte Arsiccio mine: occurrence and crystal structure. *Can. Mineral.*, **50**, 235–251.

Orlandi, P., Biagioni, C., Moëlo, Y., Bonaccorsi, E., Paar, W. (2013): Lead antimony sulfosalts from Tuscany (Italy). XIII. Protochabournéite, $\sim Tl_2Pb(Sb_{9-8}As_{1-2})_{\Sigma 10}S_{17}$, from the Monte Arsiccio mine: occurrence, crystal structure and relationship with chabournéite. *Can. Mineral.*, **51**, 475–494.

Pandeli, E., Bagnoli, P., Negri, M. (2004): The Fornovolasco schists of the Apuan Alps (Northern Tuscany, Italy): a new hypothesis for their stratigraphic setting. *Boll. Soc. Geol. It.*, **123**, 53–66.

Săbău, G. & Alberico, A. (2007): What is CCZN-armalcolite? A crystal-chemical discussion and an ad-hoc incursion in the crichtonite-minerals group. *Studia Univ. Babes-Bolyai Geologia*, **52**, 55–66.

Salje, E.K.H., Chrosch, J., Ewing, R.C. (1999): Is ''metamictization'' of zircon a phase transition? *Am. Mineral.*, **84**, 1107–1116.

Shannon, R.D. (1976): Revised effective ionic radii and systematic studies of interatomic distances in halides and chalcogenides. *Acta Crystallogr.*, **A32**, 751–767.

Sheldrick, G.M. (2008): A short history of SHELX. *Acta Crystallogr.*, **A64**, 112–122.

Vujanovic, V. (1969): Miromirite, lead-bearing davidite from Nezilovo, Macedonia. *Radovi Inst. Geol-Rudarska Istrazivanja Ispitivanya Nuklear. Drugih Mineral. Sirovina*, **5**, 147–155. (in Serbian with German summary)

Wang, D. (1981): Plumbodavidite – a new variety of davidite. *Chin. Sci. Bull.*, **26**, 915–919.

Wilson, A.J.C. ed. (1992): *International Tables for X-ray Crystallography*, volume C: mathematical, physical and chemical tables. Kluwer Academic, Dordrecht.

Wülser, P.-A., Brugger, J., Meisser, N. (2004): The crichtonite group of minerals: review of the classification. *Bull. Liaison Soc. Fr. Minéral. Cristallogr.*, **16**, 76–77.

Wülser, P.-A., Meisser, N., Brugger, J., Schenk, K., Ansermet, S., Bonin, M., Bussy, F. (2005): Cleusonite, $(Pb,Sr)(U^{4+},U^{6+})(Fe^{2+},Zn)_2(Ti,Fe^{2+},Fe^{3+})_{18}(O,OH)_{38}$, a new mineral species of the cricthonite group from the western Swiss Alps. *Eur. J. Mineral.*, **17**, 933–942.

Zhang, J., Ma, J., Li, L. (1988): The crystal structures and crystal chemistry of lindsleyite and mathiasite. *Geol. Rev.*, **32**, 132–144.

Received 15 October 2013
Modified version received 10 February 2014
Accepted 17 February 2014